ELSEVIER

Remote Sensing of Environment 80 (2002) 397–405

Remote Sensing of Environment

www.elsevier.com/locate/rse

Effects of spatial variability in light use efficiency on satellite-based NPP monitoring

David P. Turner[a,*], Stith T. Gower[b], Warren B. Cohen[c], Matthew Gregory[a], Tom K. Maiersperger[a]

[a]*Department of Forest Science, Oregon State University, Corvallis, OR 97331-7501, USA*
[b]*Department of Forest Ecology and Management, University of Wisconsin, Madison, WI 53706, USA*
[c]*USDA PNW Research Station, Corvallis, OR 97331-7501, USA*

Received 24 April 2001; received in revised form 23 August 2001; accepted 31 August 2001

Abstract

Light use efficiency (LUE) algorithms are a potentially effective approach to monitoring global net primary production (NPP) using satellite-borne sensors such as the Moderate Resolution Imaging Spectroradiometer (MODIS). However, these algorithms are applied at relatively coarse spatial resolutions (≥ 1 km), which may subsume significant heterogeneity in vegetation LUE (ϵ_n, g MJ^{-1}) and, hence, introduce error. To examine the effects of spatial heterogeneity on a LUE algorithm, imagery from the Advanced Very High Resolution Radiometer (AVHRR) at $\approx$1-km resolution was used to implement a LUE approach for NPP estimation over a 25-km^2 area of corn (*Zea mays* L.) and soybean (*Glycine max* Merr.) in central Illinois, USA. Results from several ϵ_n formulations were compared with a NPP reference surface based on measured NPPs and a high spatial resolution land cover surface derived from Landsat ETM+. Determination of ϵ_n based on measurements of biomass production and monitoring of absorbed photosynthetically active radiation (APAR) revealed that ϵ_n of soybean was 68% of that for corn. When a LUE algorithm for estimating NPP was implemented in the study area using the assumption of homogeneous cropland and the ϵ_n for corn, the estimate for total biomass production was 126% of that from the NPP reference surface. Because of counteracting errors, total biomass production using the soybean ϵ_n was closer (86%) to that from the NPP reference surface. Retention of high spatial resolution land cover to assign ϵ_n resulted in a total NPP very similar to the reference NPP because differences in leaf phenology between the crop types were small except early in the growing season. These results suggest several alternative approaches to accounting for land cover heterogeneity in ϵ_n when implementing LUE algorithms at coarse resolution.

1. Introduction

Monitoring global terrestrial net primary production (NPP) is relevant to understanding the global carbon cycle and evaluating effects of interannual climate variation on food and fiber production (Running et al., 1999). One approach to monitoring NPP employs satellite-borne sensors that achieve daily coverage over the Earth's surface at spatial resolutions of 250–1000 m, such as the Moderate Resolution Imaging Spectroradiometer (MODIS) (Justice et al., 1998). Surface reflectances derived from these sensors are used to infer the fraction of incoming photosynthetically active radiation absorbed by the vegetation (f_{APAR}) (Asrar, Fuchs, Kanemasu, & Hatfield, 1984; Goetz & Prince, 1996). The combination of f_{APAR} and an estimate of incident PAR from systems such as the Geostationary Operational Environmental Satellite (Gu & Smith, 1997) can provide an estimate of PAR absorbed by the canopy (APAR). Knowledge of the efficiency with which vegetation converts APAR into biomass (ϵ_n) then permits an estimate of NPP. Light use efficiency (LUE) models have been applied regionally (Goetz et al., 1999) and globally (Ruimy, Saugier, & Dedieu, 1994), generally with limited validation. One potential source of error in these implementations is subgrid-scale heterogeneity in ϵ_n (Behrenfeld et al., 2001).

Initial studies with crop species suggested that ϵ_n was stable across species (Montieth, 1972) and evolutionary

* Corresponding author. Tel.: +1-541-737-5043; fax: +1-541-737-1393.
E-mail address: david.turner@orst.edu (D.P. Turner).

0034-4257/01/$ – see front matter
PII: S0034-4257(01)00319-4

theory supports the convergence of ϵ_n across vegetation types (Field, 1991). However, as ϵ_n was measured for a wider variety of species and vegetation types, the earlier generalization gave way to recognition of significant variation (Goetz & Prince, 1999; Gower, Kucharik, & Norman, 1999; Ruimy et al., 1994). Climatic constraints on NPP have also been studied and have indicated greater consistency in ϵ_n if APAR is excluded from the annual sum when conditions are unfavorable for production (e.g., Runyon, Waring, Goward, & Welles, 1994). Gross primary production (GPP), the net effect of carboxylation and photorespiration, has been proposed as an alternative basis for LUE algorithms because light absorption is more directly linked to GPP than NPP, i.e., plant species differ in their allocation to autotrophic respiration (Goetz & Prince, 1999). Differences among species in foliar nitrogen concentration, which is linked to photosynthetic potential (Field & Mooney, 1986; Sinclair & Horie, 1989), and in carboxylation biochemistry—notably, the C_3 and C_4 pathways—also suggest associated differences in GPP production efficiency (ϵ_g).

To whatever degree that ϵ_n or ϵ_g do vary among vegetation cover types, it becomes important to understand effects of spatial heterogeneity in these production efficiencies on the implementation of LUE algorithms. Stands of aspen and black spruce are commonly found in close association in boreal forests, yet, they have quite different ϵ_n's (Goetz & Prince, 1996; Gower et al., 1999). C_3 and C_4 crop species are often used in rotation (e.g., wheat and lentils) and, hence, are commonly found in adjoining fields, but the crop types differ in ϵ_n (Gower et al., 1999). In these cases, assignment of ϵ_n to a coarse resolution grid cell, which includes both cover types, is problematic.

We used measurements of NPP, incident PAR, and leaf area index (LAI) to evaluate ϵ_n in adjacent corn and soybean fields in central Illinois. We also employed fine-resolution satellite imagery to assess spatial heterogeneity in crop cover type over a 25-km^2 area and develop a NPP reference data layer. Potential effects of implementing a coarse resolution LUE algorithm on NPP estimates in the area were then assessed using imagery from the Advanced Very High Resolution Radiometer (AVHRR) system.

2. Methods

2.1. Land cover

The study was performed on a 5 × 5-km area of cropland in central Illinois during 1999. The site is part of the network of eddy covariance flux towers associated with AmeriFlux (2001) and the network of Core Validation Sites associated with the MODIS Land Team (2001).

A Landsat ETM+ image dating from July 29, 1999 was acquired from the MODIS Land Team (2001) website to produce the land cover map. Source image characteristics include level 1G processing, a cell size of 30 m, and UTM (WGS84) projection. The image was subsequently resampled to 25-m resolution using a cubic convolution algorithm to match the grain size of supporting field measurements. The cosine of the solar zenith angle (COST) radiometric correction model (Chavez, 1996) was applied to convert the source image digital counts to reflectance. Since pixels falling in deep cloud shadow were found to be the darkest scene element, they were used as dark objects in the radiometric calibration algorithm. They were assumed to have 2% reflectance based on published estimates of shadowed vegetation reflectance (Adams et al., 1995; Hall, Shimabukuro, & Huemmrich, 1995). The positional accuracy of the image was digitally assessed by direct comparison with USGS digital orthophoto quadrangles (DOQs) in the study area.

Land cover mapping was performed using an unsupervised clustering of the six ETM+ reflectance bands. A *K*-means approach was used, with 30 clusters being initialized along the principal axis of variation within the six-dimensional reflectance space. The algorithm produced a set of 30 stable clusters, with a 98% convergence rate over the course of 20 iterations. Clusters were assigned to five classes: water, urban and built, barren and sparsely vegetated, corn, and soybean. This assignment was performed with reference to the DOQs, air photos, interpreter knowledge, and spectral characteristics examined in bivariate frequency distributions. Some confusion was apparent in the cluster map, most notably between the urban and built and barren and sparsely vegetated categories. Additionally, minor confusion within crop types occurred, for example, where localized drainage features reduced the separability of soybean from corn in more moist (lower reflectance) areas. Given that the spatial boundaries between confused land cover classes was readily apparent, hand digitizing and recoding was performed to eliminate the majority of spectral confusion among classes. For the purposes of this analysis, the urban and built, barren and sparsely settled, and water classes were aggregated to an "Other" class (Fig. 1).

Validation of the classification was based on the 80 points sampled for LAI and NPP (see below) plus 20 additional points distributed randomly over the 5 × 5-km area. Locations for all land cover validation points were registered to within several meters using an Ashtech GG-24 Surveyor Global Positioning System unit (Ashtech, 2001).

2.2. Net primary production

As part of a related study that compared plot-level NPP measurements to measurements of net ecosystem exchange from an eddy covariance flux tower (Reich, Turner, & Bolstad, 1999), 80 plots were established within a 1-km radius of a centrally located eddy covariance flux tower. A complete description of the sampling scheme and field measurement protocols is summarized by Campbell, Burrows, Gower, and Cohen (1999). Corn was the predominant cover type within this area, hence, a disproportionate

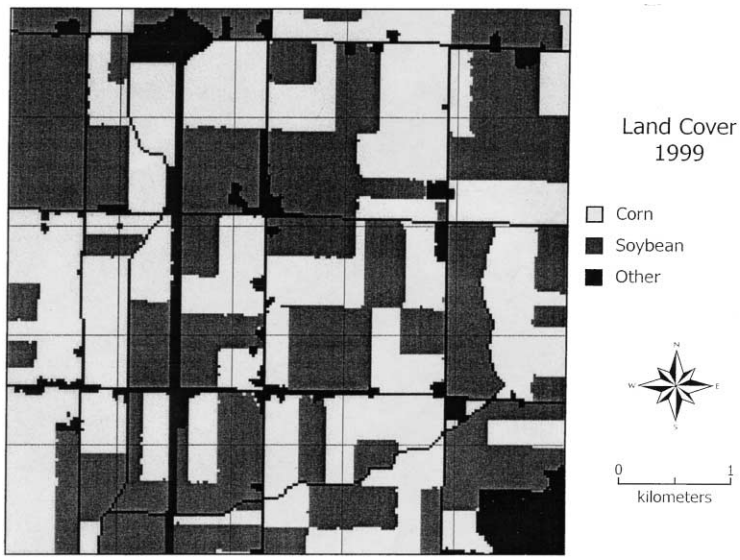

Fig. 1. Land cover data layer for the study area in 1999. The latitude and longitude at the lower right corner is 39°59′07″, 88°15′47″.

number (80%) of the plots were corn. On Day of Year (DOY) 253 in 1999, a destructive harvest was made to determine aboveground biomass. On this occasion, the density of plants was measured by direct counts of the number of stems per 5 m of row, and the number of rows per 25 m of field. One plant was then harvested from each quadrant of the 25 × 25-m plot. After drying, the average biomass per plant was scaled to the plot level by reference to the plant density. For the annual NPP estimates, biomass at DOY 253 was converted to NPP using an aboveground to total production ratio of 0.9 (Desjardins, 1985; Foth, 1962; Gower et al., 1999; Jones, Allen, Jones, Boote, & Campbell, 1984; Rochette, Desjardins, Pattey, & Lessard, 1995; Ruimy et al., 1994).

2.3. LUE by crop type

Determination of ϵ_n requires estimates of NPP and APAR. For the purposes of determining APAR, a continuous record of incident PAR and of f_{APAR} is needed. Incident PAR data was available from a meteorological station less than 5 km from the study area maintained by the SURFRAD network (SURFRAD, 2000). Half-hourly average PAR values (W m^{-2}) were converted to joules and summed over the daylight periods to develop a daily time series for 1999 (Fig. 2). A corresponding f_{APAR} time series for each crop type was derived from the LAI measurements.

The relationship of f_{APAR} to LAI has previously been studied in corn and soybeans (Daughtry, Gallo, Goward, Prince, & Kustas, 1992; Tollenaar & Bruulsema, 1988) and these relationships are of the form

$$f_{APAR} = a(1 - e^{-k \times LAI}) \quad (1)$$

where a = an empirical constant, k = extinction coefficient, and LAI = projected leaf area per unit ground area.

For this study, we developed a representative LAI time series for each crop type using field measurements and estimated daily f_{APAR} from these time series. Values for a and k (see Fig. 3) were taken from Daughtry et al. (1992).

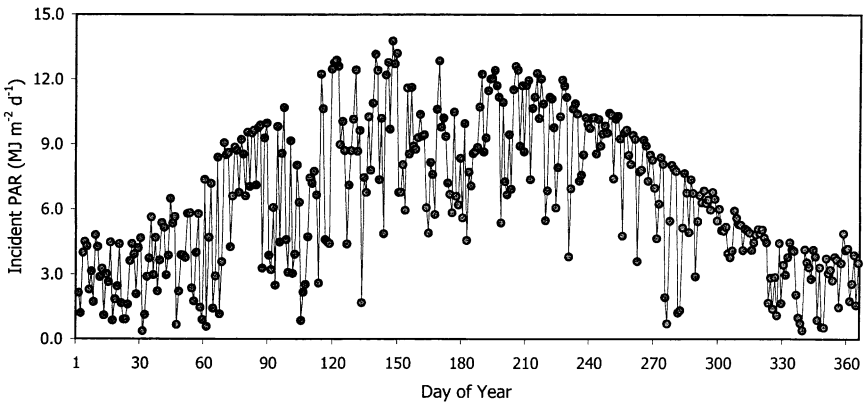

Fig. 2. Incident PAR in 1999.

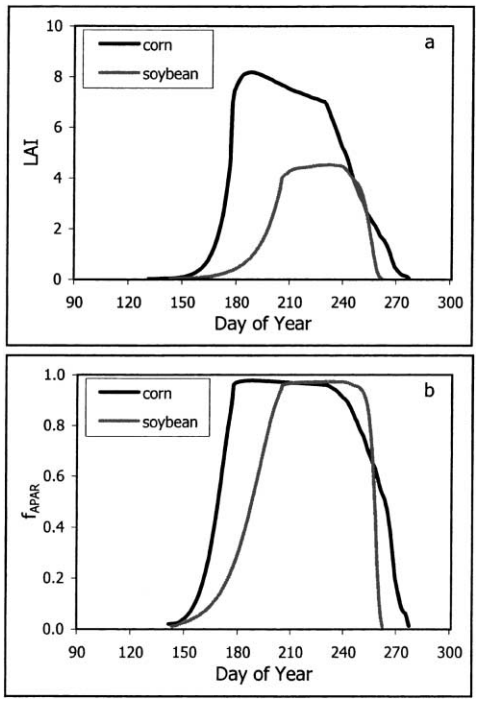

Fig. 3. Seasonal trajectories of (a) LAI and (b) f_{APAR} for corn and soybeans. The relationships of f_{APAR} to LAI (Daughtry et al., 1992) are (1) $f_{APAR}=0.976(1-e^{(-0.463\times LAI)})$ for corn and (2) $f_{APAR}=0.943(1-e^{(-0.803\times LAI)})$ for soybean.

The daily green LAI estimates were derived from LAI measurements in the early to mid-growing season at the same 80 plots used for NPP. At each of three sampling dates (DOYs 147, 173, and 208), leaves were removed from one plant representing each quadrant of each plot and passed through a leaf area meter to determine projected green leaf area per plant. As with biomass, these values were scaled to the plot level by reference to the plant density. To create a continuous representative LAI time series for each crop type, mean LAI at each sampling date for each crop type was determined and an exponential function was fit to the means at the first two LAI measurement dates when leaf biomass was present (DOYs 147 and 173 for corn and DOYs 173 and 208 for soybean). The trajectories for the latter part of the growing season were based on the third sampling date and a green LAI time series reported at the eddy covariance flux tower (Ameriflux, 2001). There, continuous measurements of incoming and reflected PAR at the flux tower were used to develop daily LAI time series for corn in 1999 and soybean in 1998 (Tilden Meyers, National Oceanic and Atmospheric Administration, personal communication). Because the soybean LAI trajectory was from 1998, it may have differed somewhat from the actual 1999 trajectory. However, neither 1998 nor 1999 were extreme climate years (e.g., in both cases, annual precipitation was within 15% of the 30-year mean), so the trend at the end of the growing season was assumed to be similar. The final representative LAI trajectories (Fig. 3a) were consistent with earlier studies that have recorded the time course of LAI development in corn and soybean (Daughtry et al., 1992; Desjardins, 1985; Gallo, Daughtry, & Wiegand, 1993; Rochette et al., 1995). The LAI trajectories were converted to f_{APAR} trajectories (Fig. 3b) by using Eq. (1). The product of daily incident PAR from the meteorological station (Fig. 2) and the daily f_{APAR} yielded a daily estimate of APAR for each crop type. ϵ_n was estimated from the total NPP and the growing season APAR.

2.4. Area-wide NPP estimates

A 1-km resolution APAR time series was created to implement a LUE algorithm over the 25-km^2 study area. The 1999 AVHRR biweekly maximum value composite of the normalized difference vegetation index (NDVI) was used for the f_{APAR} component (B. Reed, USGS EROS Data Center, personal communication). Theoretical studies have generally found a linear relationship between f_{APAR} and satellite-based spectral vegetation indices such as NDVI, with minor variation across vegetation types (Sellers, 1987; Sellers et al., 1994). To create an NDVI/f_{APAR} model specific to this study area, an estimate of f_{APAR} at the 1-km resolution was made for each AVHRR grid cell in the 5 × 5-km study area for each 2-week AVHRR composite period. Direct spatial correspondence was achieved by overlaying the 25-m land cover grid with the 1-km AVHRR grid. The coarse resolution f_{APAR} were derived by first assigning an f_{APAR} to each ETM+ resolution cropland cell for each day based on the cover type, its associated f_{APAR} time series (Fig. 3b), and the DOY. The cells in the Other class were assigned an f_{APAR} of zero. Then the average of the 1600 f_{APAR} within each 1-km cell was determined at the end of each 2-week compositing window. The end of the compositing window was used because it was most likely to match the maximum NDVI during the green-up phase of the growing season.

The time series of NDVI values for a particular cell in the AVHRR dataset is not a precise sample across time for a fixed 1-km grid cell on the ground because of the positional uncertainty of AVHRR imagery (±1 pixel) and the maximum value compositing procedure (Holben, 1986). The effect of this positional uncertainty is greatest when a 1-km area contains a significant proportion of the Other class with low NDVI. Because subgrid-scale areas of low NDVI tend not to be represented in the AVHRR time series, the three 1-km cells that had greater than 25% of their area in the Other class were not included in the development of the NDVI/f_{APAR} regression.

The resulting relationship of NDVI to f_{APAR} (Fig. 4) was used with the original NDVI time series over the complete growing season to generate the coarse resolution f_{APAR} time series. The incident PAR time series was then applied to the biweekly f_{APAR} to get the daily APAR time series at the 1-km resolution over the 25-km^2 study area.

To assess results from a coarse resolution LUE approach, NPPs were generated assuming the whole area had the ϵ_n of corn or the whole area had the ϵ_n of soybean. For a third

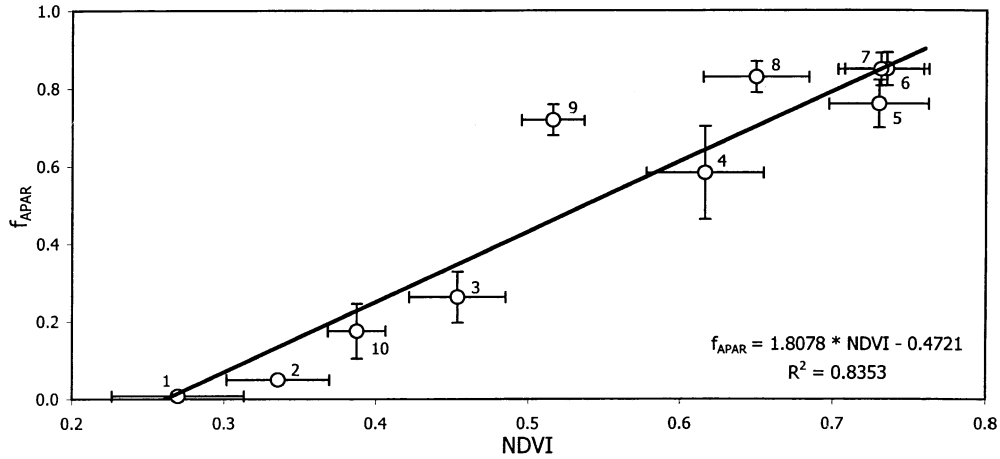

Fig. 4. The relationship over the growing season of NDVI from the AVHRR dataset and mean f_{APAR} values for the associated 1-km cells. The points are the means for the twenty-two 1-km cells used in the development of the regression and the bars indicate the S.D. The numbers are the successive 2-week compositing periods (beginning with DOY 126).

approach, the high spatial resolution land cover map was used to assign crop-specific ϵ_n. The Other class was assigned an ϵ_n of zero for this case. A NPP reference data layer was created by summing the product of area and mean NPP, as measured by the plant samples, for the two crops. The NPP of the Other class was assumed to be zero.

3. Results

Within the 25-km^2 study area, 44.4% of the land was classified as corn, 44.4% as soybean, and 11.2% as Other. Classification accuracy of the 100 validation points was 94%. Small cropped areas that site visits had revealed as being neither corn nor soybean were misclassified as corn or soybean.

The LAI measurements indicated an earlier leaf-out and a higher maximum LAI for corn than soybean (Table 1). Differences between the crops in the f_{APAR} time series were smaller than differences in the LAI time series (Fig. 3a,b). Corn reached an f_{APAR} greater than 0.9 by DOY 177 and soybean followed 25 days later. Corn f_{APAR} dropped below 0.9 on DOY 241 and soybean did so on DOY 252.

Total APAR on the biomass sampling date was 750 MJ m^{-2} for corn and 601 MJ m^{-2} for soybeans. Differences in APAR between the crop types were largest early in the growing season (Fig. 5) because of the earlier leaf-out of corn. The rate of APAR accumulation was similar between the two crop types once soybean was fully leafed out.

Table 1
Green LAI measurements at three dates

	Corn		Soybeans	
DOY	Mean	S.D.	Mean	S.D.
147	0.07	0.03	0.0	0.0
173	3.42	1.14	0.38	0.08
208	7.68	1.47	4.08	0.96

At the biomass sampling date, aboveground biomass for soybean was 55% of that for corn. Estimated NPP was 1180 (S.D. 218) g m^{-2} for soybeans and 2159 (S.D. 558) g m^{-2} for corn based on plant densities of 6.9 (S.D. 0.8) plants m^{-2} for corn and 32.5 (S.D. 2.9) plants m^{-2} for soybean. The ϵ_n for the period up to DOY 253 was 2.88 g MJ^{-1} for corn and 1.96 g MJ^{-1} for soybean.

NDVI and f_{APAR} increased in tandem over most of the growing season, then decreased late in the growing season (Fig. 4). The largest deviations between the observations and the least squares linear regression was for Periods 8 and 9 when there was a possible temporal mismatch between NDVI and f_{APAR}. The foliage was beginning to senesce during this period, with an associated increase in red reflectance but not near infrared reflectance—hence, a decrease in NDVI. The maximum value compositing procedure probably assigned a value from the beginning of the interval when the NDVI was relatively high. However, the green f_{APAR} was from the end of the period when it had been reduced because of senescence.

For the reference NPP map based on the crop-specific areas and crop-specific NPPs, the average NPP for the 25-km^2 study area was 1482 g m^{-2} and total biomass

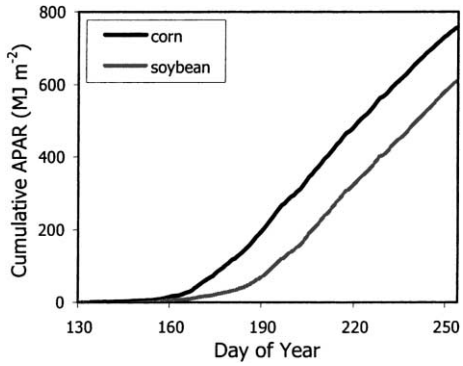

Fig. 5. Cumulative APAR for corn and soybean.

Table 2
Average NPP and total biomass production for the study area using different algorithms

Algorithm	NPP ($g\ m^{-2}$)	Total production ($g \times 10^{10}$)
Crop-specific areas and NPPs	1482	3.70
LUE model		
All corn	1873	4.68
All soybean	1281	3.20
High-resolution land cover	1403	3.51

production was 3.70×10^{10} g. With the LUE approach and the assumption of continuous corn, the estimated biomass production was 126% of the reference total (Table 2). For the set of cells that were actually corn, there was an average NPP difference of 286 $g\ m^{-2}$ between the reference value and the LUE-based value. This effect was the result of the slightly lower f_{APAR} in the early growing season relative to what it would have been had the area actually been all corn. In contrast, the actual soybean cells were overestimated by an average of 693 $g\ m^{-2}$ (a total of 0.77×10^{10} g), predominantly because ϵ_n was too high. In addition, the f_{APAR} early in the growing season was slightly higher than would be expected for an area that was uniformly soybean. The cells classed as Other were mapped as 1873 $g\ m^{-2}$ (0.52×10^{10} g). For the alternative assumption, in which the whole area was assigned a soybean ϵ_n, total biomass production was 86% of the NPP reference total. In this case, there were also compensating errors. The dominant factor was the assignment of a low ϵ_n to corn grid cells causing an average underestimate of 878 $g\ m^{-2}$ (0.97×10^{10} g). The actual soybean cells were overestimated by an average of 101 $g\ m^{-2}$ (0.11×10^{10} g) because of the slightly higher f_{APAR} early in the growing season. The assumption of production by the Other cells resulted in an overestimate of 1281 $g\ m^{-2}$ per cell (0.36×10^{10} g). When the high-resolution land cover was used to prescribe ϵ_n, with f_{APAR} from the 1-km AVHRR, total biomass production was within 5% of the reference value.

4. Discussion

The linear relationship found in this study between average green f_{APAR} within 1-km cells and NDVI from the AVHRR sensor is consistent with similar relationships for several crop species found at the plot scale with boom-mounted sensors (Gallo, Daughtry, & Bauer, 1985; Gallo et al., 1993). The slope for the satellite-based relationship was 1.8 compared to 1.2 for a plot scale study with corn and soybean (Daughtry et al., 1992). Factors such as solar-surface-sensor geometry, atmospheric effects, background effects, and nongreen biomass (Huemmrich & Goward, 1997; Myneni, Asrar, Tanre, & Choudhury, 1992) contribute to the scatter in the satellite-based NDVI/f_{APAR} relationship, but a consistent signal across the growing season was apparent. This convergence of results from plot-level studies and coarse resolution satellite imagery supports the general approach of monitoring green f_{APAR}, and, hence, APAR, over large areas with coarse resolution remote sensing (Cihlar, Chen, & Li, 1997).

Because of the positional uncertainty of the AVHRR sensor imagery, the biweekly compositing procedure used to generate large area NDVI surfaces is likely to produce an overestimate of average f_{APAR} when there is fine-scale heterogeneity in f_{APAR}, as seen here. Pixel selection in the temporal compositing procedure is likely to avoid areas with a significant proportion of nonvegetated surface. Positional accuracy for the MODIS sensor products, which are being used in the MODIS Land Science Team LUE algorithm, is expected to be on the order of 0.1 pixel instead of one pixel as for AVHRR (Justice et al., 1998). MODIS-based estimates of f_{APAR} and APAR over heterogeneous areas are therefore likely to be an improvement over AVHRR-based estimates.

For a complete NPP monitoring algorithm, the other critical component besides APAR is the production efficiency factor. ϵ_n has been well studied in crop plants because of its potential as an indicator of growth potential (Kiniry et al., 1989; Sinclair & Horie, 1989) and because crops are a suitable model system for testing some of the assumptions of LUE-based NPP algorithms (Daughtry et al., 1992; Gallo et al., 1993). Results of these earlier studies support the result here that ϵ_n can differ widely between crops, specifically corn and soybean (Daughtry et al., 1992; Gallo et al., 1985, 1993; Gower et al., 1999; Rochette et al., 1995). Thus, when corn and soybean are grown in close proximity, the assignment of an ϵ_n to a coarse resolution pixel is problematic.

The mechanistic basis for the difference in ϵ_n between corn and soybean relates in part to the differences in photosynthetic pathway: corn is a C_4 species and soybean a C_3 species. The leaf-level photosynthesis rate per unit APAR tends to be greater in C_4 than C_3 species under conditions of high light, drought, or high temperature (Ehleringer, 1978). The benefit of the C_4 pathway becomes most significant at temperatures >25 °C. Since temperature often rises about 30 °C during the growing season in the Midwest, a differential sensitivity to temperature may in part account for the higher ϵ_n for corn relative to soybean. Soybean may also have lower ϵ_n because of energy expenditures to support nitrogen-fixing bacteria. In reviews of ϵ_n, Gower et al. (1999) and Prince (1991) found highest values in C_4 species, intermediate values for non-N-fixing C_3 species, and lowest values for N-fixing C_3 species.

If corn and soybean were grown in fields that were large relative to the resolution of the satellite sensor used to monitor f_{APAR} in an operational LUE algorithm, and crop type was readily discernable by the same sensor, then an appropriate ϵ_n could be assigned to each crop and production estimates could be made based on APAR and an associated land cover map. However, the principal implication of this study is that a LUE-based NPP algorithm run over the Midwest at coarse resolution (≥ 1 km) would be

compromised by the high spatial heterogeneity in ϵ_n. The 640-acre (2.6×10^6 m^2 or 259 ha) sections, which are the original units of ownership and management in the Midwest region, are now generally broken up into several smaller management units (Fig. 1). Consequently, 1-km^2 grid cells are often mixtures of crop types. For the 25-km^2 area of this study, the area-wide estimate for total NPP was a factor of 1.26 higher when the corn ϵ_n was used exclusively rather than the soybean ϵ_n.

Important subkilometer scale heterogeneity in ϵ_n is likely to be found in a variety of other vegetation types and land management schemes. Subgrid-scale mixtures of patches with deciduous or coniferous species, as is common in New England forests, would potentially result in relatively large errors because ϵ_n usually differs significantly between conifer and deciduous species (Goetz & Prince, 1998; Gower et al., 1999). More generally, observations of NPP in forest stands of different ages have found reductions in NPP as stand age increases (Gower, McMurtrie, & Murty, 1996; Ryan, Binkley, & Fownes, 1997). Although decreasing LAI, and, hence, f_{APAR}, is a possible cause in some cases, f_{APAR} usually remains high, thus stand ϵ_n is decreasing as NPP is decreasing (Hunt, 1994; Saldarriaga & Luxmore, 1991). In the conifer forests of the Pacific Northwest, the scale of the clearcuts over much of the public lands has been relatively small (<40 ha), such that any given 1-km^2 pixel is likely to contain patches of several ages (Turner, Cohen, & Kennedy, 2000). As with corn and soybean, the average ϵ_n for a grid cell in the Pacific Northwest region will therefore differ greatly from the ϵ_n at any particular point.

One possible approach to accounting for subgrid-scale heterogeneity in ϵ_n when employing a coarse-scale LUE algorithm would be to accept the coarse-scale APAR and use higher-resolution imagery such as Landsat ETM+ for high-resolution land cover maps when assigning ϵ_n. This approach assumes synchrony in f_{APAR} phenology, and, hence, APAR, within a coarse resolution grid cell, but permits ϵ_n of the subgrid polygons to vary. For the corn and soybean in this study, growing season APAR was 25% higher in corn but ϵ_n was 47% higher in corn. Thus, a significant component of the error associated with coarse resolution LUE analysis could be eliminated if ϵ_n were known at finer resolution.

To implement this approach in mixed C_3/C_4 croplands, a new land cover surface would be needed each year because of crop rotation. Thus, a primary operational constraint to implementing a hybrid LUE algorithm in these areas would be the need to annually update the crop cover map. Although corn and soybean were readily classified in this study, factors such as different planting dates within a crop type, similarities in reflectance among crop types, and the assembly and interpretation of multiple ETM+ scenes would present challenges in broader applications.

If the proportion of total area in each crop type was stable over time within a region, use of a weighted average ϵ_n might be another alternative to basing the regional ϵ_n on one crop type. This approach would work well in regions such as the Midwest with simple two-crop rotation schemes. For the 25 km^2 examined in this study, the area of corn and soybean were equal and together they represented a large proportion of the landscape.

LUE algorithms based on ϵ_g rather than ϵ_n (Goetz & Prince, 1998, 1999; Landsberg & Waring, 1997) would reduce the problem of subgrid-scale heterogeneity in some cases. ϵ_g has greater similarity across cover types than ϵ_n because the differences among cover types in allocation to autotrophic respiration (e.g., forest vs. grassland) are not a factor. However, the issue of estimating autotrophic respiration, which is required to estimate NPP, remains. The assumption that a constant proportion of GPP is allocated to autotrophic respiration (Waring, Landsberg, & Williams, 1998) has been questioned (Medyn & Dewar, 1999). The MODIS Land Science Team NPP algorithm (Justice et al., 1998) is based on ϵ_g but uses land cover classification both in assigning a ϵ_g to each cell and as part of the estimation of autotrophic respiration. Since the approach requires classification, the basic obstacles to implementing it in situations with fine-scale heterogeneity in vegetation cover remain.

5. Conclusions

Corn and soybean fields occur in close proximity over a large area of the Midwestern USA, yet, ϵ_n differs significantly between them. Thus, implementation of a LUE approach at coarse-resolution for NPP monitoring in this region is problematic. Since annual APAR differences between the crop types are smaller than ϵ_n differences, a possible hybrid scheme that employs both fine-resolution cover mapping and coarse-resolution monitoring of f_{APAR} may be feasible. Alternatively, a weighted average ϵ_n over a large area might be employed.

Acknowledgments

This research was funded by the NASA Terrestrial Ecology Program. We thank Tilden Meyers (Oak Ridge National Laboratory) for the use of the Bondville flux tower LAI data. The Bondville flux tower site is supported by the NOAA. The PAR measurements were from the SURFRAD network, which is likewise supported by the NOAA. Special thanks to Brad Reed (USGS EROS Data Center) for the 1999 AVHRR NDVI time series.

References

Adams, J. B., Sabol, D. E., Kapos, V., Filho, R. A., Roberts, D. A., Smith, M. O., & Gillespie, A. R. (1995). Classification of multispectral images based on fractions of endmembers: application to land-cover change in the Brazilian Amazon. *Remote Sensing of Environment*, *52*, 137–154.

AmeriFlux (2001). Available at: http://cdiac.esd.ornl.gov/programs/ameriflux/.

Ashtech (2001). Ashtech precision products. Available at: http://www.ashtech.com/.

Asrar, G., Fuchs, M., Kanemasu, E. T., & Hatfield, J. L. (1984). Estimating absorbed photosynthetic radiation and leaf area index from spectral reflectance in wheat. *Agronomy Journal*, *76*, 300–306.

Behrenfeld, M. J., Randerson, J. T., McClain, C. R., Feldman, G. C., Los, S. O., Tucker, C. J., Falkwoski, P. G., Field, C. B., Frouin, R., Esaias, W. E., Koplber, D. D., & Pollack, N. H. (2001). Biospheric primary production during an ENSO transition. *Science*, *291*, 2594–2597.

Campbell, J. L., Burrows, S., Gower, S. T., & Cohen, W. B. (1999). *BigFoot: characterizing land cover, LAI, and NPP at the landscape scale for EOS/MODIS validation*. Field Manual Version 2.1. Oak Ridge, TN: Environmental Sciences Division, Oak Ridge National Laboratory, 104 pp.

Chavez, P. S. (1996). Image-based atmospheric corrections — revisited and improved. *Photogrammetric Engineering and Remote Sensing*, *62*, 1025–1036.

Cihlar, J., Chen, J., & Li, Z. (1997). Seasonal AVHRR multichannel data sets produced for studies of surface–atmosphere interactions. *Journal of Geophysical Research, 102*, 29625–29640.

Daughtry, C. S. T., Gallo, K. P., Goward, S. N., Prince, S. D., & Kustas, W. P. (1992). Spectral estimates of absorbed radiation and phytomass production in corn and soybean canopies. *Remote Sensing of Environment*, *39*, 141–152.

Desjardins, R. L. (1985). Carbon dioxide budget of maize. *Agricultural and Forest Meteorology*, *36*, 29–41.

Ehleringer, J. R. (1978). Implications of quantum yield differences on the distribution of C_3 and C_4 grasses. *Oecologia*, *31*, 255–267.

Field, C., & Mooney, H. A. (1986). The photosynthesis–nitrogen relationship in wild plants. In: T. J. Givish (Ed.), *On the economy of plant form and function* (pp. 25–55). Cambridge: Cambridge University Press.

Field, C. B. (1991). Ecological scaling of carbon gain to stress and resource gain. In: A. Mooney, & W. E. Winner (Eds.), *Response of plants to multiple stresses* (pp. 35–65). San Diego, CA: Academic Press.

Foth, H. D. (1962). Root and top growth of corn. *Agronomy Journal*, *54*, 49–52.

Gallo, K. P., Daughtry, C. S. T., & Bauer, M. E. (1985). Spectral estimation of absorbed photosynthetically active radiation in corn canopies. *Remote Sensing of Environment*, *17*, 221–232.

Gallo, K. P., Daughtry, C. S. T., & Wiegand, C. L. (1993). Errors in measuring absorbed radiation and computing crop radiation use efficiency. *Agronomy Journal*, *85*, 1222–1228.

Goetz, S., Prince, S. E., Goward, S. N., Thawley, M. M., Small, J., & Johnston, A. (1999). Mapping net primary production and related biophysical variables with remote sensing, application to the BOREAS region. *Journal of Geophysical Research, 104* (27), 719–727, 734.

Goetz, S. J., & Prince, S. D. (1996). Remote sensing of net primary production in boreal forest stands. *Agricultural and Forest Meteorology*, *78*, 149–179.

Goetz, S. J., & Prince, S. D. (1998). Variability in carbon exchange and light utilization among boreal forest stands: implications for remote sensing of net primary production. *Canadian Journal of Forest Research*, *28*, 375–389.

Goetz, S. J., & Prince, S. D. (1999). Modeling terrestrial carbon exchange and storage: evidence and implications of functional convergence in light-use efficiency. *Advances in Ecological Research*, *28*, 57–92.

Gower, S. T., Kucharik, C. J., & Norman, J. M. (1999). Direct and indirect estimation of leaf area index, f_{APAR} and net primary production of terrestrial ecosystems. *Remote Sensing of Environment*, *70*, 29–51.

Gower, S. T., McMurtrie, R. E., & Murty, D. (1996). Aboveground net primary production decline with stand age: potential causes. *Trends in Ecology and Evolution*, *11*, 378–382.

Gu, J., & Smith, E. A. (1997). High resolution estimates of total solar and PAR surface fluxes over the BOREAS study area from GOES measurements. *Journal of Geophysical Research*, *102*, 29685–29706.

Hall, F. G., Shimabukuro, Y. E., & Huemmrich, K. F. (1995). Remote sensing of forest biophysical structure using mixture decomposition and geometric reflectance models. *Ecological Applications*, *5*, 993–1013.

Holben, B. N. (1986). Characteristics of maximum-value composite images from temporal AVHRR data. *International Journal of Remote Sensing*, *11*, 1417–1434.

Huemmrich, K. F., & Goward, S. N. (1997). Vegetation canopy PAR absorptance and NDVI: an assessment for ten tree species with the SAIL model. *Remote Sensing of Environment*, *61*, 254–269.

Hunt Jr., E. R. (1994). Relationship between woody biomass and PAR conversion efficiency for estimating net primary production from NDVI. *International Journal of Remote Sensing*, *15*, 1725–1730.

Jones, P., Allen Jr., L. H., Jones, J. W., Boote, K. J., & Campbell, W. J. (1984). Soybean canopy growth, photosynthesis, and transpiration responses to whole-season carbon dioxide enrichment. *Agronomy Journal*, *76*, 633–637.

Justice, C. O., Townshend, J. R. G., Defries, R., Riy, D. P., Hall, D. K., Salomonson, V. V., Privette, J. L., Riggs, G., Strahler, A., Lucht, W., Myneni, R. B., Knyazikhin, Y., Running, S. W., Nemani, R. R., Wan, Z., Huete, A. R., van Leeuwen, W., Wolfe, R. E., Giglio, L., Muller, J., Lewis, P., & Barnsley, M. J. (1998). The Moderate Resolution Imaging Spectroradiometer (MODIS): land remote sensing for global change research. *IEEE Transactions on Geosciences and Remote Sensing*, *36*, 1228–1249.

Kiniry, J. R., Jones, C. A., O'Toole, J. C., Blanchet, R., Cabelguenne, M., & Spanel, D. A. (1989). Radiation-use efficiency in biomass accumulation prior to grain-filling for five grain-crop species. *Field Crops Research*, *20*, 51–64.

Landsberg, J. J., & Waring, R. H. (1997). A generalized model of forest productivity using simplified concepts of radiation-use efficiency, carbon balance and partitioning. *Forest Ecology and Management*, *95*, 209–228.

Medyn, B. E., & Dewar, R. C. (1999). Comment on the article by R.H. Waring, J.J. Landsberg and M. Williams relating net primary production to gross primary production. *Tree Physiology*, (On-line).

MODIS Land Team (2001). Available at: http://modarch.gsfc.nasa.gov/MODIS/LAND/VAL/.

Montieth, J. L. (1972). Solar radiation and production in tropical ecosystems. *Journal of Applied Ecology*, *9*, 747–766.

Myneni, R. B., Asrar, G., Tanre, D., & Choudhury, B. J. (1992). Remote sensing of solar radiation absorbed and reflected by vegetated land surfaces. *IEEE Transactions on Geosciences and Remote Sensing*, *30*, 302–314.

Prince, S. D. (1991). A model of regional primary production for use with coarse resolution satellite data. *International Journal of Remote Sensing*, *12*, 1313–1330.

Reich, P. B., Turner, D. P., & Bolstad, P. (1999). An approach to spatially-distributed modeling of net primary production (NPP) at the landscape scale and its application in validation of EOS NPP products. *Remote Sensing of Environment*, *70*, 69–81.

Rochette, P., Desjardins, R. L., Pattey, E., & Lessard, R. (1995). Crop net carbon dioxide exchange rate and radiation use efficiency in soybean. *Agronomy Journal*, *87*, 22–28.

Ruimy, A., Saugier, B., & Dedieu, G. (1994). Methodology for the estimation of terrestrial net primary production from remotely sensed data. *Journal of Geophysical Research*, *99*, 5263–5283.

Running, S. R., Baldocchi, D. D., Turner, D. P., Gower, S. T., Bakwin, P. S., & Hibbard, K. A. (1999). A global terrestrial monitoring network integrating tower fluxes, flask sampling, ecosystem modeling and EOS satellite data. *Remote Sensing of Environment*, *70*, 108–128.

Runyon, J., Waring, R. H., Goward, S. N., & Welles, J. M. (1994). Environmental limits on net primary production and light use efficiency across the Oregon transect. *Ecological Applications*, *4*, 226–237.

Ryan, M. G., Binkley, D., & Fownes, J. H. (1997). Age-related decline in forest productivity: pattern and process. *Advances in ecological research*, *vol. 27* (pp. 213–262). New York: Academic Press.

Saldarriaga, J. G., & Luxmore, J. (1991). Solar energy conversion efficien-

cies during succession of a tropical rain forest in Amazonia. *Journal of Tropical Ecology*, *7*, 233–242.

Sellers, P. J. (1987). Canopy reflectance, photosynthesis, and transpiration: II. The role of biophysics in the linearity of their interdependence. *Remote Sensing of Environment*, *21*, 143–183.

Sellers, P. J., Tucker, C. J., Collatz, G. J., Los, S. O., Justice, C. O., Dazlich, D. A., & Randall, D. A. (1994). A global 1×1 NDVI data set for climate studies: Part 2. The generation of global fields of terrestrial biophysical parameters from the NDVI. *International Journal of Remote Sensing*, *15*, 3519–3545.

Sinclair, T. R., & Horie, T. (1989). Leaf nitrogen, photosynthesis, and crop radiation use efficiency: a review. *Crop Science*, *29*, 90–98.

SURFRAD (2000). Available at: http://www.srrb.noaa.gov/surfrad/surfpage.htm.

Tollenaar, M., & Bruulsema, T. W. (1988). Efficiency of maize dry matter production during periods of complete leaf area expansion. *Agronomy Journal*, *80*, 580–585.

Turner, D. P., Cohen, W. B., & Kennedy, R. E. (2000). Alternative spatial resolutions and estimation of carbon flux over a managed forest landscape in western Oregon. *Landscape Ecology*, *15*, 441–452.

Waring, R. H., Landsberg, J. J., & Williams, M. (1998). Net primary production of forests: a constant fraction of gross primary production? *Tree Physiology*, *18*, 129–134.